Periodica Polytechnica
Civil Engineering

59(2), pp. 109–122, 2015
DOI: 10.3311/PPci.7860

RESEARCH ARTICLE

Application and Assessment of Equivalent Linear Analysis Method for Conceptual Seismic Retrofit Design of Háros M0 Highway Bridge

József Simon, *László Gergely* Vigh, *Adrián* Horváth, *Pál* Pusztai
Received 07-12-2014, revised 09-01-2015, accepted 13-01-2015

Abstract

In this study, seismic performance of the existing M0 Háros Highway Bridge in Hungary is evaluated. The large-span bridge is designed with minimal consideration of seismic actions, seismic resistance of certain piers, bearings and pile foundations is not adequate. Eight different demand mitigation methods are evaluated considering quasi-elastic configurations as well as non-linear systems adopted with non-linear anti-seismic devices (NLASD). To accelerate the preliminary design phase, an equivalent linear analysis (ELA) methodology is worked out. Keeping in mind the limitations of the ELA method, non-linear time-history analysis (NLTHA) is also applied for the retrofitted configuration for validation purposes. Comparison of the two methods shows that the ELA method gives the designer adequate, still conservative results for optimal retrofit decisions.

Keywords

Continuous steel and composite bridge · seismic analysis · multi modal response spectrum analysis · time history analysis · retrofitting · non-linear displacement-dependent seismic device · equivalent linear analysis

József Simon
Budapest University of Technology and Economics, Department of Structural Engineering, H-1111 Budapest, Műegyetem rkp. 3-9., Hungary
e-mail: simon.jozsef@epito.bme.hu

László Gergely Vigh
Budapest University of Technology and Economics, Department of Structural Engineering, H-1111 Budapest, Műegyetem rkp. 3-9., Hungary
e-mail: vigh.l.gergely@epito.bme.hu

Adrián Horváth
Főmterv Civil Engineering Designer Inc., H-1024 Budapest, Lövőház utca 37., Hungary
e-mail: horvath.adrian@fomterv.hu

Pál Pusztai
CÉH Planning, Developing and Consulting Inc., H-1112 Budapest, Dió utca 3-5., Hungary
e-mail: pusztai@ceh.hu

1 Introduction

Prior to the introduction of the European structural codes – Eurocode 8 Part 1 [1] and Eurocode 8 Part 2 [2] – , bridges in Hungary were conventionally designed with no or minimal consideration of seismic loads. In 2006 a new seismic hazard map [3] was released with an increased seismic proneness, classifying Hungary as moderate seismic zone. Experiences on newly erected structures in the last decade [4, 5], and parametric studies on typical continuous girder bridges [6] indicate that large portions of typical girder bridges may be vulnerable to earthquake loads even in moderate seismic regions. In order to achieve sufficient seismic performance, critical details and elements may have to be reinforced even though they would be safe in ultimate limit state (ULS) considering conventional load effects.

In this paper, an existing highway bridge – a typical continuous girder – over the Danube River for the M0 Highway at Háros is examined. The bridge was built in 1990 and designed in accordance with the relevant Hungarian standards, the earlier version of ÚT 2-3.401 [7], without consideration of seismic actions. The Hungarian National Infrastructure Development Center plans to replace the composite girder of the river bridge due to the ageing of the concrete. The replacement results in a new structure, thus seismic performance has to be evaluated according to the the operative national standard, EC8-2.

Conventional multi-modal response spectrum analysis (MMRSA) is applied to compute probable internal forces and displacements for the existing configuration. Since some piers and bearings do not satisfy the standard seismic requirements [1, 2], seismic retrofit is needed. The main goal of the conceptual seismic retrofit design is to keep the original piers and foundations, and to achieve a cost-effective solution. There are two alternatives: 1) conventional retrofit methods strengthening the critical members; 2) mitigation of the seismic demand. The first approach leads to increased demands on construction materials, human resources and thus to significant expenses assigned to strengthening of immersed piers and foundations. On the contrary, an effective demand mitigation method may assure to keep the original substructure in its existing form. Such methods can be: a) using more sophisticated modeling

techniques (e.g. taking into account the actual, cracked pier stiffness); b) rearrangements of internal forces by replacing the fixed bearings; c) using non-linear anti-seismic devices (NLASD) such as non-linear displacement or velocity dependent seismic devices or seismic isolators to isolate the substructure from the superstructure. All these solutions could be investigated easily during the analysis, and the application of NLASDs does not require relatively high additional costs, since their construction can be implemented during the replacement of the girder. Accordingly, eight demand mitigation methods are evaluated and compared to each other on the level of internal forces in the critical elements.

The conceptual design is carried out as follows. The preliminary calculations are done with MMRSA, where elements with non-linear behavior (e.g. NLASDs) are taken into account with their effective stiffness and effective damping ratios. This method is commonly referred as equivalent linear analysis (ELA). ELA requires an iterative procedure to obtain compatible secant stiffness, forces and deformations. After finding an optimal solution, the retrofitted configuration is analyzed by non-linear time-history analysis (NLTHA) modeling the NLASDs with non-linear characteristic. The analysis results are then compared and the feasibility of the ELA is evaluated.

Comparison of NLTHA and ELA has been studied and the accuracy of the ELA method has already been evaluated by several researchers: Iwan and Gates [8], Hwang and Sheng [9], Hwang [10], Hwang et al.[11], Franchin et al. [12], Dicleli and Buddaram[13], Jara et al. [14], Simon and Vigh [15], Liu et al. [16], Zordan et al. [17]. However, these studies focus on the comparison of the two analysis methods and on the analysis of an equivalent single degree of freedom (SDOF) system of the example bridges, assuming regular layout (e.g. the pier heights are equal) and medium span lengths (under 50 m). Since the assumption of an SDOF system is generally valid in the longitudinal direction these studies do not pan out about the analysis in the transverse direction. In our study, NLASDs are applied and ELA is carried out not only in the longitudinal but also in the transverse direction, and ELA is used for the analysis of a large-span (over 100 m) existing bridge with non-regular layout to evaluate conceptual retrofit versions in a fast and efficient way.

Limitation of the ELA method is also emphasized in the above mentioned references (also see Section 3.1.2), however in spite of the limited accuracy, linearization method to determine the effective stiffness and equivalent damping of NLASDs suggested by EC8-2 and EN 15129 [18] is applied in this study. The paper focuses on the standard analysis methods provided by EC8-2, and the comparison between ELA and NLTHA is made to reveal the feasibility of the ELA for conceptual seismic retrofit design.

2 Bridge description

The total length of the bridge is 770.42 m with spans of 3 x 73.5 m (left flood bridge), 3 x 108.5 m (river bridge) and 3 x 73.5 m (right flood bridge) as it can be seen in the longitudinal view of the structure (Fig. 1a). The total width of the deck is 21.80 m (2 x 1.9 m of sidewalk and 18.0 m of carriageway). The river bridge shares two common piers with the flood bridges (pier P4 and P7) and is separated from the flood bridges by a ±70 mm and a ±160 mm expansion joint, respectively. The expansion joints applied at the abutments have a capacity of 70 mm. In the longitudinal direction the girder of the river bridge is restrained at pier P5, while the flood bridges are longitudinally fixed on pier P2 and P9. The cross sections and reinforcements of the river bridge piers are identical to that of the pier P5 (Fig. 1b). It is worth mentioning that reinforcement ratio of the piers is very low (only 0.12%). The piers of the flood bridges (P2, P3, P8 and P9) are similar constructions (also with low reinforcement ratio), however the cross sections are generally smaller, overall dimensions at the pier bottom are 11.5 m x 1.6 m. The river bridge is a continuous three-span girder with a one-cell box cross-section with inclined webs and orthotropic deck (Fig. 1c), while the flood bridges are three-span continuous composite bridges with similar dimensions.

3 Numerical modeling and analysis techniques

3.1 Equivalent linear analysis

3.1.1 Linearization method and iteration procedure

ELA uses linearization method to model the behavior of non-linear elements such as NLASDs. The behavior of the most commonly applied NLASDs (lead rubber bearings, friction based bearings, high damping rubber bearings, buckling restrained braces (BRBs) etc.) can be approximated with bi-linear characteristic (Fig. 2a), as suggested by EN15129 and EC8-2. The required parameters are: initial stiffness (K_e), the post-yield stiffness (K_p) and the yielding strength (F_y). The equivalent linear characteristic is expressed through the effective stiffness (K_{eff}) and effective damping (ξ_{eff}) of the device. In accordance with EC8-2, ELA can be carried out with an iteration procedure. The calculation of the effective damping ratio provided by EC8-2 is identical to the suggestion by AASHTO [19] based on the work of Jacobsen and Ayre [20]. Fig. 2b shows the flowchart of the iteration procedure. Elastic acceleration response spectrum should be used as per EC8-1. In each iteration step, MMRSA is completed using K_{eff} of the non-linear components and ξ_{eff} of the overall system. With the obtained deformations the effective properties are updated for the subsequent iteration steps. In the i^{th} iteration step, the actual deformation $d_{bd,i}$ of a seismic device is computed as:

$$d_{bd,i} = \frac{F_{calc,i}}{K_{eff,i}} , \tag{1}$$

where $F_{calc,i}$ is the calculated force in the NLASD. Once the actual deformation is known, the corresponding compatible force $F_{act,i}$ (lying on the original bi-linear curve) can be determined:

$$F_{act,i} = F_y + K_p \left(d_{bd,i} - d_y \right) , \tag{2}$$

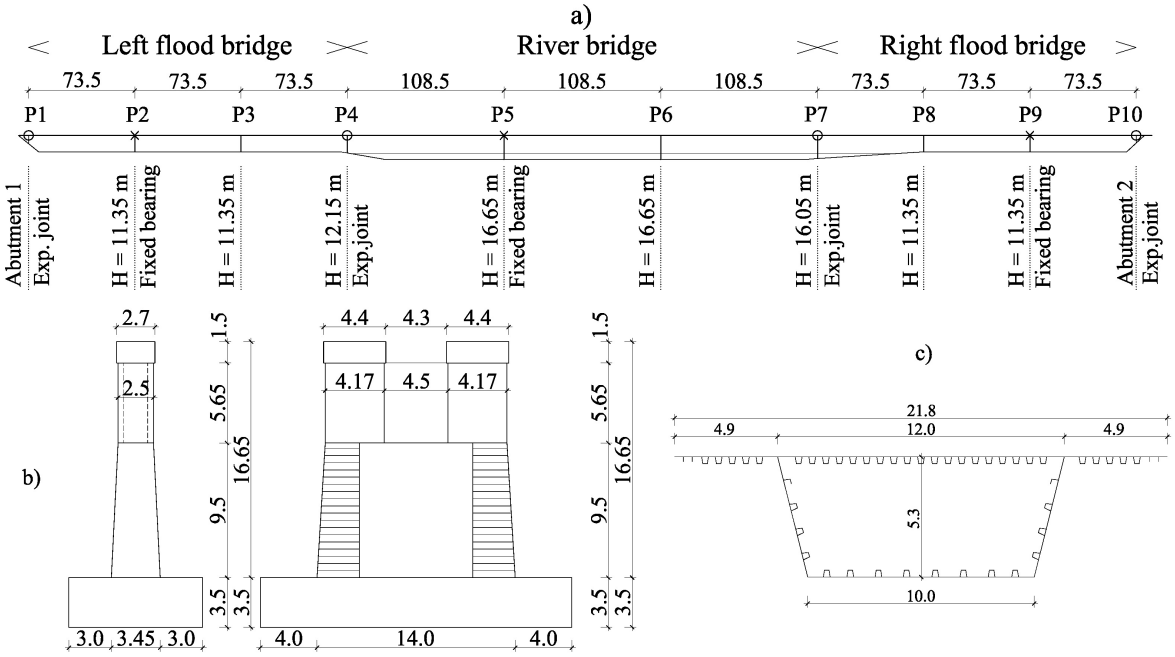

Fig. 1. Configuration of the existing bridge. a) side-view of the bridge; b) side-views of pier P5; c) cross-section of the river bridge girder.

assuming that $d_{bd,i}$ is greater than d_y. The updated effective stiffness ($K_{eff,i+1}$) is defined as the secant stiffness corresponding to the actual calculated deformation level:

$$K_{eff,i+1} = \frac{F_{act,i}}{d_{bd,i}} \,. \tag{3}$$

In each iteration step the effective damping ratio $\xi_{eff,i+1}$ is calculated from the actual deformation ($d_{bd,i}$) and the effective damping of the whole system ($\xi_{eff,s,i+1}$) should be defined. The effective damping of one isolator unit can be described by the following equation according to EC8-2:

$$\xi_{eff} = \frac{4\left(F_y - K_p d_y\right)\left(d_{bd} - d_y\right)}{2\pi K_{eff} d_{bd}^2} \,. \tag{4}$$

Reliable estimation of the effective damping of the whole system ($\xi_{eff,s}$) is crucial in the analysis. Damping of the unisolated bridge can be taken into account through material damping of the piers and the superstructure, and can be estimated by the structural type and material properties. Adding NLASDs, the local damping of each device makes the system unproportionally damped, thus the classical modal analysis cannot be carried out, the model properties become complex-valued. There are different approaches to solve this problem such as complex modal analysis [21], composite damping rule [22] or simply neglecting off-diagonal elements in the damping matrix. However, practical analysis is complicated by the fact that these methods require additional analyses or computational capacity that most commercial design softwares do not provide. According to Feng and Lee [23], the theoretical maximum value of $\xi_{eff,s}$ is the sum of the effective damping of each seismic device plus the assumed 5% material damping of the structure. In our investigation $\xi_{eff,s}$ is calculated from the sum of the effective damping of the isolator units, while the material damping of the structure is neglected. The elastic response spectrum curve shown in Fig. 2c incorporates the effect of damping of the whole system via the modification factor $\eta_{eff,i}$ [1]:

$$\eta_{eff,i} = \sqrt{\frac{10}{5 + \xi_{eff,s,i}\,[\%]}} \,. \tag{5}$$

The iteration then should be continued until the difference in $d_{bd,i}$ and $d_{bd,i+1}$ is less than 5%.

3.1.2 Limitations of the equivalent linear method

As listed in Section 1, the accuracy of the ELA method has already been evaluated by several researchers. These studies were carried out using Eq. (4) to determine the effective damping ratio. It is concluded that the determination of the effective damping is critical and in several cases it is overestimated. The accuracy of the internal forces are often not sufficient, the error can be as high as 20 to 30% in some cases. Evaluating the accuracy of the ELA, several new formulations were proposed by various authors, which are based on either modifying the original equation [13, 16, 17, 24], or creating formulae considering datasets from non-linear analyses [8, 14, 25].

In [13], a comprehensive study of the accuracy of the ELA based on the original Eq. (4) formula was carried out. New conclusions were made that the accuracy depends not only on the ductility ratio of the seismic device (μ), but the effective period of the structure (T_{eff}) and the frequency characteristics of the ground motion such as the peak ground acceleration to peak ground velocity ratio (A_p / V_p), as well. It was also concluded that the error of approximation is higher if the A_p / V_p ratio is higher and the effective period of the structure is lower. According to the results, the underestimation of the internal forces can be as high as 20 - 30% compared to NLTHA.

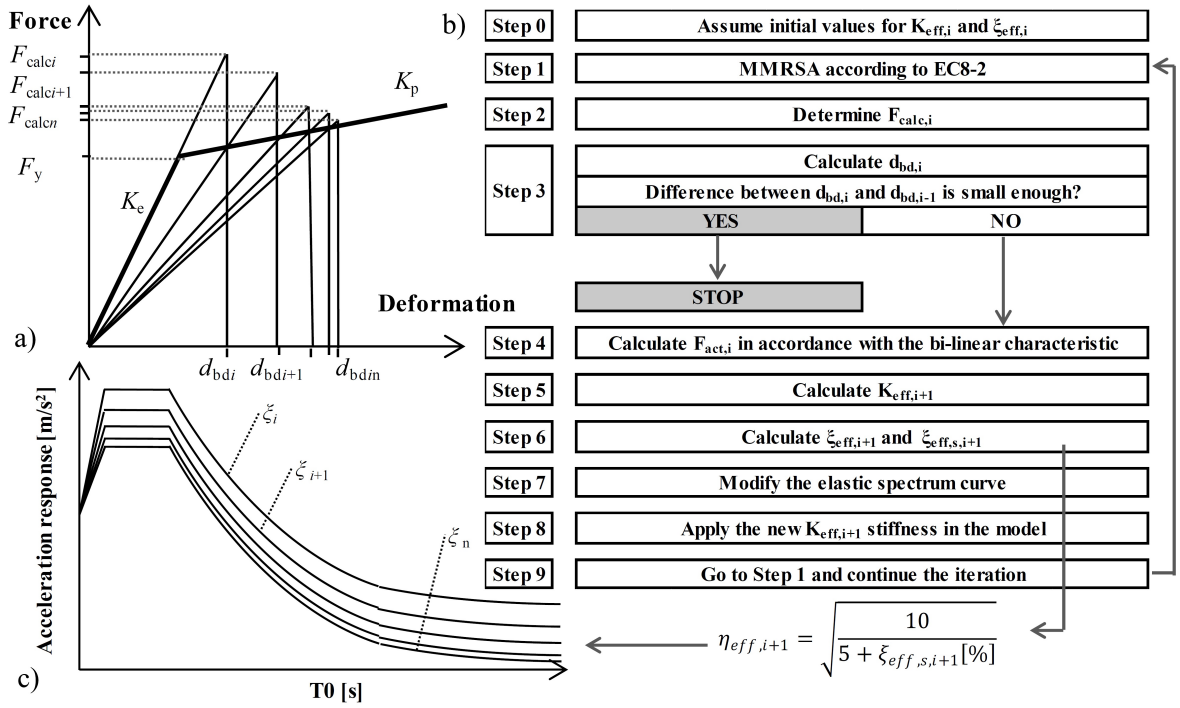

Fig. 2. Flowchart of the iteration procedure for equivalent linear analysis: a) bi-linear approximation of the behavior of NLASDs; b) steps of the iteration procedure; c) modification of the standard acceleration response spectrum (T0 denotes the natural period in [s]).

In [15], the feasibility of the ELA was investigated through three typical continuous girder bridge examples. The analysis was carried out by iterative MMRSA and NLTHA using artificial acceleration records in accordance with EC8-1. It was concluded that these records generally have an excessive number of cycles of strong motion, so the A_p / V_p ratio and thus the approximation error of the ELA as per the conclusions of [13] could be high as 20 - 30%.

Considering this observation and results of previous studies, the determination of effective damping formula suggested by EC8-2 should be also revised. As a conclusion, the error resulted from the application of effective system damping cannot be neglected in preliminary ELA for conceptual retrofit design of the existing highway bridge. Thus, the computed internal forces are approximately increased by a factor of 1.3 in resistance verifications. Despite of the above uncertainty, application of ELA is beneficial due to its fast computational time providing the opportunity of fast analysis of various alternatives.

3.2 Time-history analysis

Linear (LTHA) and non-linear (NLTHA) time-history analyses are also applied in this study. LTHA is used for the analysis of the existing configuration (see Section 4.2) expecting lower seismic demands by the application of time-domain based analysis rather than frequency-based. The reason of using NLTHA is to reliably capture the realistic hysteretic behavior of non-linear components. The advanced analysis bridges over the above-discussed shortcomings (see Section 3.1.2) of the simplified ELA, as the energy dissipation is modeled directly. In the present study, NLTHA is used for the analysis of the retrofitted configuration and for comparison with the iterative MMRSA used in ELA (see Section 6.1 and 6.2).

Since in Hungary, there is a lack of recorded strong motions, a new, iterative algorithm is developed in Matlab [26] to create artificial acceleration records determined to fit the 5%-damped elastic response spectrum as it is proposed in EC 8-1 for time-history analysis. The artificial input consists of a set of sinusoidal waves, the algorithm changes the amplitude of these waves in each iteration step untill the response of the artificial input fits the standard spectrum with an error less than a predefined value. A detailed explanation of the artificial record generation algorithm can be found in [5]. In line with the standard provisions, seven artificial records are used in both directions, then the average of the results from seven analyses is calculated in accordance with EC 8-1. The applied artificial records and their acceleration response spectra as well as the applied standard acceleration spectrum can be seen in Fig. 3.

4 Numerical model

A three dimensional beam-element numerical model is developed in ANSYS FEM software [27]. A schematic picture of the numerical model can be seen in Fig. 4. The main structure, the girder and the piers are modeled by two-node 3D beam elements with 6 degree of freedoms (DOFs) per node. The beam elements are placed in the center of gravity, and eccentricity between the member axis – such as axis of the superstructure and bearings placed on pier top – is bridged over by the help of rigid elements. The same rigid elements are used to model the eccentricity of the pier foot and pile cap. The bearings on the piers and the abutments are modeled by zero-length elements with linear

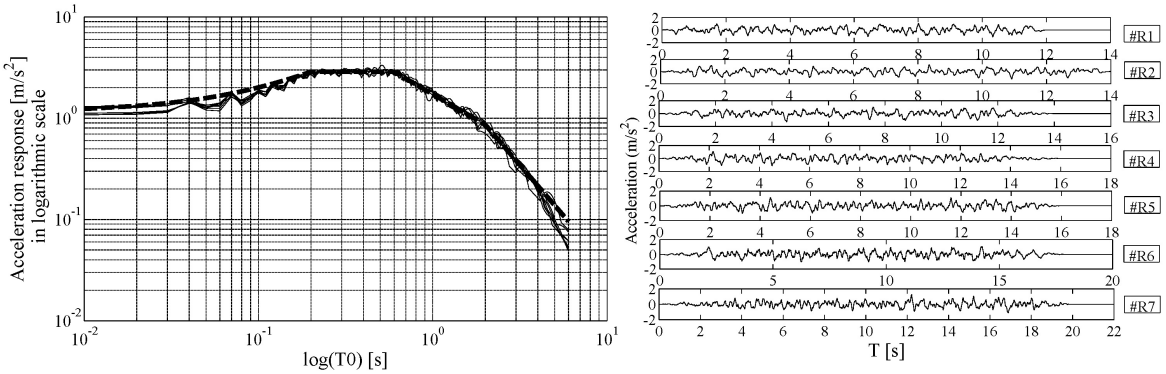

Fig. 3. Applied seven artificial acceleration records and their response spectra, compared to the standard response spectrum used in the ELA.

or non-linear spring characteristics – depending on the analysis type – assigned to three translational degrees of freedom (u_x, u_y, u_z), but rotations are free to develop. A typical mesh size of one meter along girder length and pier height results in approximately 550 nodes (~ 3300 DOFs), which is found sufficient to efficiently achieve results with an acceptable accuracy. Different material models are assigned to the elements depending on the analysis type.

Linear model (LM) is used for linear MMRSA and LTHA. In this case, geometric and material non-linearity is ignored. Accordingly, both the girder and the piers are modeled with elastic beam elements. Steel and concrete members are adjusted with a Young modulus value of 210 and 32 GPa, respectively. According to Hungarian design practice, fixed bearings are considered fully rigid, while expansion bearings provide no restraint in the model. In each restrained translational direction a linear spring stiffness of 10^{13} N/m is adjusted to the fully rigid connections. When NLASDs are applied in the ELA, they are represented by linear springs with effective stiffness values (generally ranging from $3.5 \cdot 10^7$ to $2.5 \cdot 10^9$ N/m). The soil-structure interaction at the foundations of the piers is taken into consideration with integrate linear springs, adjusted with stiffness values (Table 1) calculated from foundation analysis.

Non-linear model (NLM) is applied for NLTHA. The only difference between the LM and NLM is that the applied NLASDs in the final retrofitted configuration are modeled by zero-length elements with bi-linear hysteretic material model approximation (see Fig. 2a).

Tab. 1. Effective spring stiffness values reflecting soil-structure interaction.

Pier #	k_x MN/m	k_z MN/m	k_{xx} MNm/rad	k_{zz} MNm/rad
P 2-3, P 8-9	3570	4810	55560	250000
P4, P7	4760	5130	111000	350000
P5, P6	3850	4550	125000	500000

Note: k_x and k_z are the transverse and longitudinal translational stiffnesses, respectively; k_{xx} and k_{zz} are the transverse and longitudinal rotational stiffnesses, respectively.

5 Seismic vulnerability of the existing bridge

5.1 Response spectrum analysis

The seismic analysis of the existing configuration is carried out by MMRSA, in accordance with EC8-2. The parameters of the standard acceleration response spectrum curve are: $a_g = 1.0\,\text{m/s}^2$, soil type C, type 1 spectrum, damping ratio $\xi = 0.05$. The applied mass is calculated from the dead loads of the girders and an additional $1.0\,\text{kN/m}^2$ live load distributed on the carriageway which leads to an equivalent distributed load of 14.9 t/m along the length of the girder. The total seismic mass of the system – including piers, foundation heads – is approximately 41000 t.

Typical modal shapes and the computed periods are summarized in Fig. 5 and in Table 2. Approximately 100 modes are required to satisfy the 90% modal mass rule in each direction. Mode 2, 4 and 5 with fundamental periods of 0.91, 0.81 and 0.75 s represent the longitudinal movement of the left and right flood bridges and the river bridge respectively, activating 45% of the total mass, representing the mass of the superstructure and

longitudinally restrained piers (P2, P5 and P9). Thus it means that the whole bridge is in movement in the longitudinal direction except for the piers with expansion bearings.

The first transverse movements appear in the 11th mode (fundamental period of 0.44 s) with girder movements only and thus an activated mass of only 4%. The more dominant mode in this direction is mode 15 (fundamental period of 0.35 s) where the activated mass is nearly 38% due to the contribution of the movements of the piers as well. It can be seen that the fundamental periods of the modes in the transverse direction are lower than the T_c period value (0.6 s) – representing the edge of the plateau of the applied response spectrum –, thus high base shear forces are expected.

According to the MMRSA results, the girders are found to be adequate. The maximum hogging and sagging moments are 198.04 and 140.76 MNm in case of the river; and 160.53 and 138.89 MNm in case of the flood bridges, respectively. The maximal deflections of the left flood and the river bridges are 103 and 263 mm, and are developed dominantly from dead load. However, the transverse and longitudinal displacements of the girders are driven by the seismic action. The longitudinal dis-

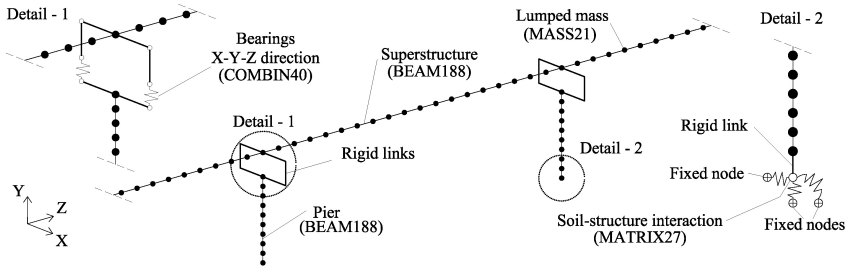

Fig. 4. Details of the global numerical model.

Tab. 2. Modal frequencies, fundamental periods and modal mass ratio values of the existing configuration (version V1).

Mode #		1	2	3	4	5	6	7	8	9	10	11	12	13	14	15
f	Hz	0.87	1.10	1.12	1.23	1.34	1.50	1.51	1.63	1.76	1.76	2.25	2.31	2.31	2.50	2.86
T	s	1.16	0.91	0.89	0.81	0.75	0.67	0.66	0.61	0.57	0.57	0.44	0.43	0.43	0.40	0.35
m_x	-	0.00	0.00	0.00	0.00	0.00	0.00	0.00	0.01	0.00	0.00	4.01	0.01	0.01	0.12	37.63
m_y	-	1.12	0.01	0.00	0.05	0.20	1.51	1.57	8.50	0.00	0.00	0.00	10.38	10.26	0.00	0.01
m_z	-	0.20	15.09	0.27	14.56	16.05	0.24	0.74	0.24	0.08	0.04	0.00	0.01	0.00	0.00	0.00

Note: m_x. m_y and m_z are the modal mass ratio (ratio of effective mass to total mass) values in the transverse, vertical and longitudinal direction, respectively.

placements of the left flood, river and right flood bridges are 40, 38 and 35 mm, respectively. In the transverse direction, the displacements are quite low (8 and 8 mm in the case of the left and right, and 27 mm in the case of the river bridges) which is the consequence of the higher bridge stiffness in this direction. The demand on expansion joints are 55, 130, 148 and 50 mm at the left abutment, pier P4, pier P7 and right abutment. The expansion joints are adequate at the abutments (with a capacity of ±70 mm) and at pier P7 (with a capacity of ±160 mm), however, at pier P4 the device is likely to fail due to its low capacity of only ±70 mm designed for only thermal action. These joints can be replaced during the replacement of the original superstructure, thus the new design should be carried out taking into consideration these results.

Representative results of internal forces for the bearings and the piers are summarized in Table 3. The maximal transverse forces are 6111, 7791 and 6671 kN in case of the left flood, river and right flood bridges. The difference in height between the shared piers (P4 and P7) results in different bearing forces in pier P3 and P8. The longitudinal bearing forces are higher than 5500 kN in every case, the maximal value is 6210 kN calculated at pier P5 of the river bridge. For comparison, the breaking force calculated in ULS is 1170 kN. This means that the bearing forces in the longitudinal direction is increased at least 4 - 5 times due to the seismic action.

Similarly, great increase is induced in the bending moments of both directions. The maximal values are obtained at the pier P5 of the river bridge: 198.50 and 254.10 MNm around the longitudinal (M_z) and transverse axis (M_x), respectively. In Table 3, normal forces calculated in quasi-permanent combination are also illustrated. These values are used to determine the biaxial bending capacity of the piers. For the capacity evaluation and comparison of the subsequent bridge configurations, and because longitudinal actions are dominant, demand-to-capacity (D/C) ratio is computed as the ratio of the design bending moment (increased with second order effects) in the longitudinal direction and the corresponding bending resistance. The bending resistance is calculated from the segment of the M_x - M_z - N interaction surface at the given design transverse bending moment. According to the capacity analysis, the most critical piers are those with fixed bearing in the longitudinal direction, the D/C ratio of the most critical pier P5 is 4.19.

As a conclusion of the seismic analysis, the critical structural components are the longitudinally restrained piers P2, P5 and P9 with their foundations, and the fixed bearings in the longitudinal direction. Although, the expansion joints can be replaced during the construction of the new superstructure, the seismic action should be taken into consideration while choosing appropriate devices, and if possible, the seismic retrofit design should be carried out minimizing the seismic demand on these joints.

5.2 Linear time-history analysis

MMRSA overestimates the occurring internal forces when several vibration modes contribute. To quantify the level of overestimation, LTHA is further invoked. Fig. 6 compares the bending moments on the foundations, computed from MMRSA and LTHA. The figure confirms that in comparison to MMRSA results, the actual internal forces are lower, e.g. at pier P5 the differences are 15% and 39% in the longitudinal and transverse directions, respectively. The fact that the differences between MMRSA and THA results are higher in the transverse direction is in line with the expectations: in the longitudinal direction one dominant mode shape characterizes the seismic behavior. One can observe that high decrease (greater than 50%) of internal forces are obtained in the longitudinal direction in case of the longitudinally non-restrained piers (P3, P4, P6, P7 and P8). This stems from the fact that the Rayleigh damping is adjusted

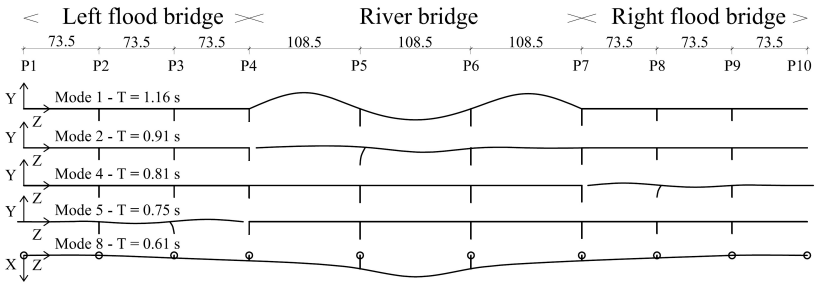

Fig. 5. Dominant mode shapes and corresponding fundamental periods of the existing configuration.

Tab. 3. Representative results (bearing forces and pier internal forces) from the MMRSA of the existing bridge.

Pier #		P1	P2	P3	P4		P5	P6	P7		P8	P9	P10
Component			<Left flood bridge >				<River bridge >				<Right flood bridge >		
							Bearing forces						
F_x	kN	1701	6111	6099	1785	1642	7791	7173	1991	2277	4664	6671	1769
F_z	kN	-	5550	-	-	-	6210	-	-	-	-	6024	-
							Pier internal forces						
M_z	MNm	-	100.64	100.34	55.93		198.50	182.00	105.66		81.67	101.97	-
M_x	MNm	-	136.11	6.85	21.09		254.10	49.91	39.82		8.16	137.02	-
N	kN	-	26000	26143	25067		33109	33006	27855		26521	25891	-

Note: F_x and F_z are the bearing forces in kN in the transverse and longitudinal direction, respectively. M_x, M_z are the maximal pier moments in MNm around the transverse and longitudinal global axes, N is the normal force of the pier in kN calculated from quasi-permanent loads.

to the dominant first two modes which are not in correspondence with the higher natural frequencies of the individual piers. This numerical issue should be taken into consideration during the design of individual piers if only LTHA with Rayleigh damping is applied. However, in our case, results from the MMRSA can be used for safety check.

The resistance verification indicates that the critical piers P2, P5 and P9 are still not capable to resist the mitigated seismic demands. The D/C ratio for instance is 2.89 in case of the most critical pier P5.

6 Equivalent linear analysis for conceptual seismic retrofit design

6.1 Demand mitigation methods

Because seismic resistance of the existing structure is not adequate, intervention into the structural performance is necessary. Conventional strengthening of the critical members is extremely complicated by the fact that pier P5 is embedded in water, thus cross-section strengthening and foundation re-piling is very costly. To survey cost-effective solutions, the next phase of the conceptual design considers simple structural rearrangements (e.g. number of fixed bearings) as well as the applicability of advanced seismic retrofit techniques using seismic isolation system. Table 4 lists the set of 9 different arrangements for the evaluation – including the original version –, illustrating the evolution of conceptual design. The layouts are chosen in the aspect that the cost-consuming pier and foundation strengthening should be avoided.

6.2 Results of the ELA method

The conceptual retrofit design is carried out applying ELA with the iteration procedure presented in Section 3.1. Note that: firstly, the internal forces of the girders from seismic action are likely to be lower than those from ULS; secondly, the foundations are assumed to be designed consistently with the piers, thus it is expected that if the capacity of the adjacent pier is not exceeded, the foundation is adequate as well. Accordingly, in the remainder of the paper, the results of these components are not presented in detail. To illustrate the steps of the conceptual design, representative results are presented in four figures. Longitudinal and transverse bending moments acting in the bottom section of the piers are compared in Fig. 7. Additionally, Fig. 8 presents the D/C ratios for the critical river bridge piers P5, P6 and P7 (the piers of the flood bridges are found to be adequate, since the longitudinal fixed bearings are removed and placed to the abutments), while the bi-axial bending interaction diagram of the most critical pier P5 is depicted in Fig. 9. Finally, to demonstrate the global behavior of the structure the transverse and longitudinal displacements as well as the demand on the expansion joints of pier P4 and P7 are also presented in Fig. 10 in a normalized form to show the difference between the actual and the original, existing configuration.

6.2.1 Version V2 - effect of actual pier stiffness

As a first step, the effect of actual pier stiffness on the seismic response is investigated in version V2. In this case the stiffness of the cracked cross section is estimated according to EC8-2, and the original stiffness is decreased by a factor of 0.5. Taking into account the effective stiffness of the piers, significant

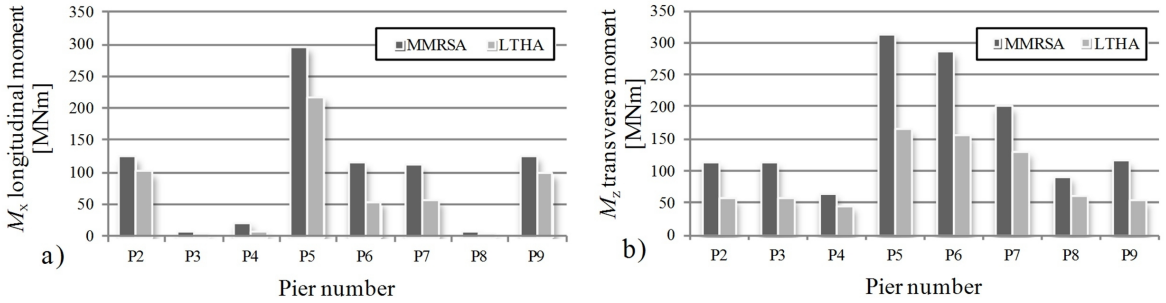

Fig. 6. Comparison of pier foundation bending moments in the existing configuration from MMRSA and from LTHA.

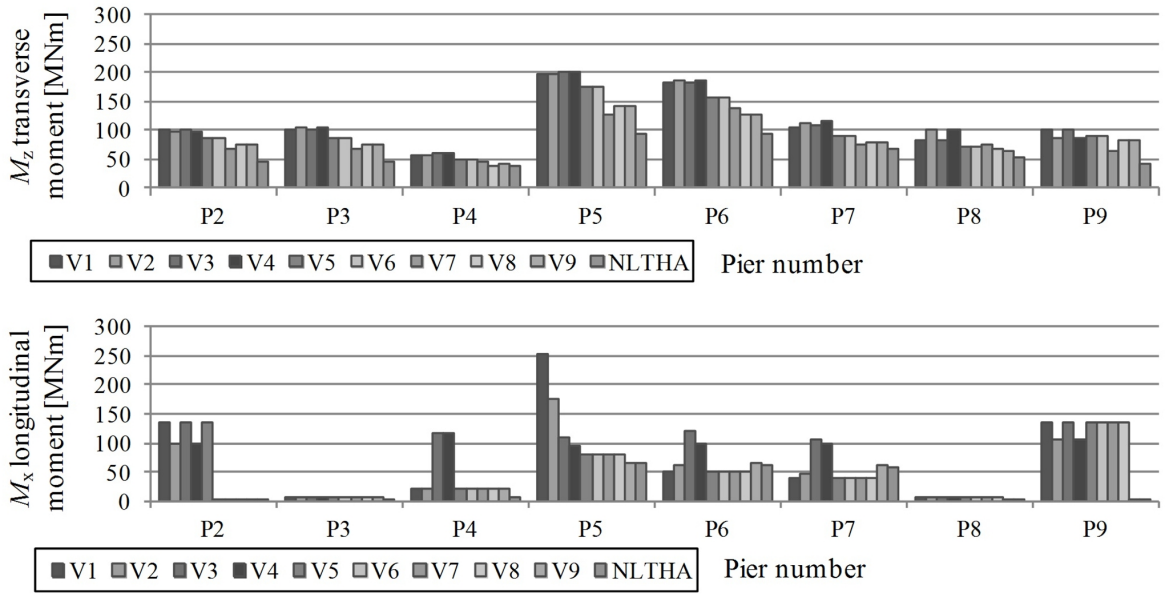

Fig. 7. Pier bending moments in piers, calculated from the ELA of the nine examined configurations and from the NLTHA of the retrofitted version V9.

decrease of the longitudinal moments of the longitudinally fixed piers can be observed in the existing configuration (Fig. 7). The M_x moments are reduced by 26 - 30 - 23% at pier P2, P5 and P9, respectively, however, the D/C ratio of the most critical pier P5 is still over 1.0 with a value of 2.97 (Fig. 8). Noteworthy increase in bending moments of the free-standing piers is also obtained. For instance, this increase is 24% at pier P6 and 22% at pier P7. Due to their relatively small effective mass and high stiffness in the longitudinal direction, short period – falling within the initial ascending branch of the acceleration spectrum (e.g. $T < T_c$) – characterizes these piers. The consideration of cracking decreases the pier stiffness, while increases the fundamental period, leading to increased seismic forces. Since relatively high uncertainty can be adjusted to the modeling of actual rigidity and masses and the developing seismic force is very sensitive to this change in this region of the spectrum curve, the authors suggest that the plateau value of the spectrum should be conservatively applied in the very short period range. In this version no noticeable change in the transverse moments (M_z) can be observed (Fig. 7).

The increased flexibility causes higher displacements, thus higher demands on the expansion joints as well. Fig. 10 indicates a 23% increase of the longitudinal displacement of the

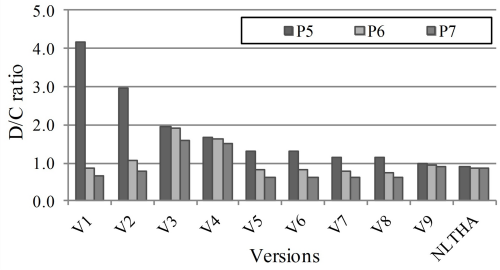

Fig. 8. Demand-capacity (D/C) ratios calculated for pier P5, P6 and P7 in case of the ELA of the nine examined configurations and from the NLTHA of the final retrofitted version V9.

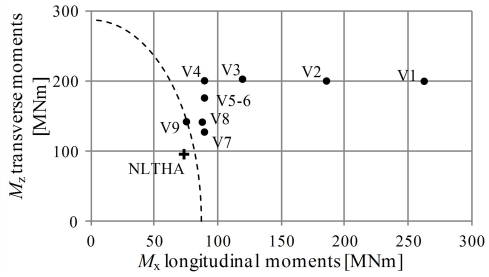

Fig. 9. Bi-axial bending interaction diagram, transverse and longitudinal pier bending moments for pier P5 in case of the ELA of the nine examined configurations and from the NLTHA of the final retrofitted version V9.

Tab. 4. Applied layouts for demand mitigation methods.

Ver.	Dir.	Ab.	Piers										Ab.	Pier stiffness
		P1	P2	P3	P4/1	P4/2	P5	P6	P7/1	P7/2	P8	P9	P10	
1	*z*		+				+					+		100%
	x	+	+	+	+	+	+	+	+	+	+	+	+	
2	*z*		+				+					+		50%
	x	+	+	+	+	+	+	+	+	+	+	+	+	
3	*z*		+			+	+	+	+			+		100%
	x	+	+	+	+	+	+	+	+	+	+	+	+	
4	*z*		+			+	+	+	+			+		50%
	x	+	+	+	+	+	+	+	+	+	+	+	+	
5	*z*		+				I1					+		100%
	x	+	+	+	+	+	+	+	+	+	+	+	+	
6	*z*	I1					I1						I1	100%
	x	+	+	+	+	+	+	+	+	+	+	+	+	
7	*z*	I1					I1						I1	100%
	x	+	+	+	+	+	I3	I3	+	+	+	+	+	
8	*z*	I1					I1						I1	100%
	x	+	+	+	+	+	I3	I3	I4	I5	+	+	+	
9	*z*	I1					I1	I1	I1				I1	100%
	x	+	+	+	+	+	I3	I3	I4	I5	+	+	+	

Note: *z* – longitudinal; *x* – transverse direction. I1, I2, I3, I4 and I5 are reference numbers to the applied isolator properties (refer to Table 5).
"+" signs denote fixed bearings in the applied directions.

river bridge girder, causing higher demands on the expansion joint of pier P4 with 18%. In the transverse direction, the increase is lower, around 7% in case of displacements of the river bridge girder.

6.2.2 Version V3-V4 - rearrangements of internal forces

In version V3 the longitudinally fixed bearings are rearranged to study how the seismic loads can be re-distributed between the piers of the river bridge (P4, P5, P6 and P7) placing fix bearings in the longitudinal direction. In this way, significant decrease of the internal forces in the critical pier P5 can be reached, the M_x moments are nearly equally distributed to a level of 115.0 MNm. However, the newly involved piers are drastically overloaded. The total base shear force of the bridge is 1.7 times larger than in the previous cases due to the larger rigidity provided by the additionally involved piers. Due to this larger rigidity, the longitudinal displacements are significantly lower, 48% compared to the existing configuration, resulting in lower demand with a 16% decrease of the expansion joints as well. The calculated D/C ratios are 1.9 in case of the river bridge piers. This means that the same demand level can be reached with the rearrangements of the internal forces, however, this decrease is still not sufficient.

In version V4, the effect of actual pier stiffness is also investigated in this configuration (version V3). The M_x bending moments are decreased in the piers, moments around 95.0 MNm are obtained. This results 1.65 D/C ratios for pier P4, P5, P6 and P7.

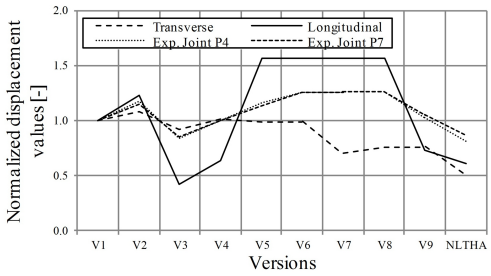

Fig. 10. Transverse and longitudinal displacements of the river bridge girder; seismic demand on the expansion joints of pier P4 and P7. Values are normalized by those of the original configuration to represent the difference in the original and current version.

6.2.3 Version V5-V6 - applying NLASDs in the longitudinal direction

The above-discussed approaches (version V2-V4) cover wide variety of possible traditional interventions in the quasi-elastic system. It is concluded that quasi-elastic system cannot yield to sufficient seismic performance. Straightforward solution is the application of seismic NLASD as seismic isolator units between the piers and superstructure in order to limit the internal forces transferred from the superstructure to the substructure. In version V5, the longitudinally fixed bearings on pier P4, P6, P7 are removed, and the longitudinally fixed bearings between pier P5 and the superstructure are replaced with NLASD seismic devices with 1200 kN nominal yield resistance (F_y). Selection of the nominal yield resistance is based on the concept that the seismic device shall work in the elastic range in serviceability and ultimate limit states (SLS and ULS), i.e. yielding occur due to seismic event only. The initial stiffness (K_e) is chosen sufficiently high to prevent excessive displacements caused

by strong wind effects, traffic loads, thermal loads or moderate earthquakes. The post to initial stiffness ratios ($\alpha = K_p / K_e$) are around 0.05, representing either lead rubber bearings, or special devices such as BRBs or hydraulic dampers with properly chosen characteristics. These assumptions are valid for all the NLASDs applied in this study. The required NLASD properties are listed in Table 5. The reference numbers of the applied devices are also indicated in Table 4. Versions where NLASDs are applied, the decreased stiffness of the piers due to cracking is neglected: due to the large uncertainties in stiffness estimations, the internal force analyses are carried out with 100% piers stiffness, as conservative estimates.

Tab. 5. Characteristics and reference numbers of the applied NLASDs.

	#No	I1	I2	I3	I4	I5
F_y	kN	1200	3300	5100	1815	1650
K_e	kN/mm	250	1400	2200	750	700
K_p	kN/mm	15	75	115	40	40

The application of the devices beneficially reduces the bending moments in pier P5, approximately to the same level as in version V4 (the decrease of M_x is 68%), besides, the original – low – load intensities on the other piers (pier P4, P6 and P7) are obtained. However, the D/C ratio of pier P5 is still 30% over of the desired value 1.0.

The longitudinal displacement of the girder is increased from 37 to 58 mm compared to the existing configuration due to the deformation of the applied NLASD. The calculated bearing force is 1465 kN, causing the NLASD to yield to a deformation of 23 mm. The higher longitudinal displacements are reflected in the demand on the expansion joints. However, the increase is lower, only 16% at pier P4 since the displacement of the flood bridges are unchanged.

In version V6, the cost-efficient retrofit of the flood bridges are examined, this version does not affect the river bridge compared to version V5. The layout is chosen by recognizing the benefits of placing the fixed bearings in the longitudinal direction from pier P2 and P9 to the abutments. However, the calculated reaction forces transferred to the abutments are excessive and they should be limited by applying NLASDs with properly chosen characteristic to avoid the cost-consuming strengthening. Thus, instead of fixed bearings NLASDs with nominal yield resistance of 1200 kN are placed to the abutments in version V6. It can be seen in Fig. 7 that the M_x moments are lowered to the level of the other piers of the flood bridges. Applying NLASDs increases the displacements of the flood bridges to 53 mm. Accordingly, the demands on the expansion joints are higher with 26% compared to the existing configuration, the demand is 187 mm at pier P7, for instance.

In version V6, the demands of the flood bridges in the most critical longitudinal direction are transferred from the piers to the abutments, thus the D/C ratio of the piers are unlikely to be over 1.0. Accordingly, the remainder of the paper deals with the presentation of the results of the river bridge only.

6.2.4 Version V7-V8 - applying NLASDs in the transverse direction

Moments in the transverse direction are not changed significantly in the previous versions. In case of the river bridge, these moments also have to be decreased with NLASDs for sufficient performance. Two arrangements are evaluated regarding the position of the isolator bearings in the lateral direction: isolators placed on only the two middle piers (P5 and P6) in version V7 or on the river bridge piers P5, P6 and P7 in version V8. Decrease of the moments of pier P5 is higher with the first layout, but regarding all river bridge piers, the second approach is more favorable. The moments of the P4, P5, P6 and P7 pier are mitigated by 18 - 36 - 24 - 28% in the first, and 28 - 29 - 30 - 24% in the second case, respectively. However, the D/C ratio of pier P5 is still over 1.0 with a value of 1.16 in the latter case. In spite of applying NLASDs, the maximal transverse displacements of the river bridge girder are decreased by 30 and 24%, respectively. However it should be noted that these are low displacement values (ranging from 20 to 27 mm).

6.2.5 Final version V9

Since the critical pier P5 does not have sufficient reserve capacity against the expected higher internal forces obtained from NLTHA – MMRSA results increased by a factor of 1.3 –, a similar approach as it can be seen in version V3 is applied. Internal forces in the longitudinal direction are distributed to pier P6 and P7 as well, but in this case NLASDs are used to minimize the force transferred from the superstructure to the piers and thus the bending moments of the piers. On the originally non-restrained pier P6 and P7 shock-transmission units are also applied constituting a series system with the NLASDs to allow girder movements for quasi-static loads like thermal actions. With this layout, the moments in the river bridge piers with the same load bearing capacity (pier P5, P6 and P7) can be modified to be on the same level, the longitudinal M_x moments are 66.9, 66.0 and 61.78 MNm, while the D/C ratios are 0.99, 0.95 and 0.91 at pier P5, P6 and P7, respectively. Involving further piers to the vibration results in stiffer structure in the longitudinal direction, leading to lower displacements. Compared to the existing configuration, the longitudinal displacements are decreased by 26%, although it is higher than in the case of version V3 where the decrease is high as 58%. Demands on the expansion joints are slightly higher than in the existing configuration, 133 and 156 mm at pier P4 and P7, meaning only 2 and 5% increase, respectively.

7 Non-linear time-history analysis of the retrofitted configuration

7.1 Results of the NLTHA

NLTHA of the final version V9 is carried out with NLM presented in Section 3.3, using seven different artificial records fit

to the standard response spectrum curve. Design values of internal forces and deformations are computed as the average results of the seven analyses. Demonstration of the seismic behavior of the bridge is implemented through two figures.

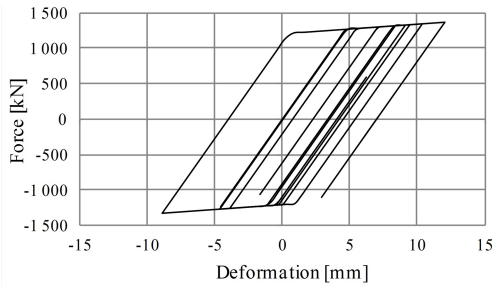

Fig. 11. Force-deformation diagram of the NLASD applied at pier P5 in the longitudinal direction using artificial record #R1. Characteristics of the device can be seen in Table 5.

Fig. 11 illustrates the force-deformation diagram of the NLASD on pier P5, obtained from artificial acceleration record #R1. Due to hardening of the NLASD device, the bearing force on pier P5 is higher by 13% compared to the nominal yielding force (F_y). Longitudinal displacements of the girder of the river bridge from LTHA of the existing version V1, and NLTHA of the retrofitted version V9 is presented in Fig. 12a. According to the results the dominant natural period is not elongated significantly. As per the modal analysis the natural period of the existing configuration is 0.75 s, while that of the retrofitted version calculated with MMRSA with effective stiffness is 0.80 s. This is due to including more piers in the vibration and increasing the stiffness of the vibrating system. Despite of this, the combined effect of the natural period elongation and the damping of the isolators results smaller displacements of the girder compared to the original version. However, due to the yielding of the NLASD, residual displacements can be observed in the retrofitted version, but this displacement is insignificant, only 6 mm. The longitudinal moments in pier P5 can be also seen in Fig. 12b. The maximum moment in the critical pier P5 is 208.4 MNm in the existing configuration, and can be mitigated to 62.5 MNm with the final retrofit version. The D/C ratios are 0.90, 0.88 and 0.87, slightly different than in the case of the ELA (see comparison in the following Section 6.2). The reduction in displacements are higher, 49 and 39% compared to the existing configuration. This is significantly different than the results of ELA. Demands on expansion joints are also decreased regarding the original values of version V1. The decrease is 19 and 13% at per P4 and P7, respectively.

7.2 Comparison of the two analysis methods

Comparison of the ELA and NLTHA is implemented by presenting five different responses in both horizontal directions at pier P5, P6 and P7, and by evaluating the differences of the results shown in Table 6. The screened values are: internal force and deformation of the NLASD; girder displacement; pier top displacement and pier moment in each examined direction. For pure comparison, results from ELA are presented in Table 6 without applying the 1.3 increasing factor for the internal forces.

Observing the results in the longitudinal direction, one can conclude that the force in the NLASD can be approximated by ELA method with negligible error. This is due to the bi-linear characteristic and low post-yield stiffness (i.e. low kinematic hardening behavior) of the device. However in case of pier moments, deformations and displacements the accuracy of ELA is not sufficient as expected. The error is generally around 20 - 30% compared to the NLTHA which is considered to be the exact solution. The deformation of the NLASD and thus the girder displacements are overestimated by 16 - 31%, while the pier top displacements are underestimated by 7 to 21%. This underestimation is reflected in the pier moments: typically 20% larger internal forces obtained by NLTHA. These results are in accordance with Section 3.1.2 and the conclusions of [13] and [15].

In the transverse direction, the results are less consistent: under- and overestimation of the screened values can be also observed. All screened values are higher from the ELA compared to the NLTHA in case of pier P5 and P6. This means, that even though the equivalent damping ratios are overestimated, applying time-history analysis leads to lower demands. The tendency is the opposite at pier P7, but the maximal overestimation is not higher than 26% (pier top displacement), and lower than 10% in case of the internal forces (NLASD force, pier moment).

The results can be possibly explained as follows. Even in case of the longitudinal direction, it is hard to tell the level of under- or overestimation. This stems from the fact that the uncertainty of the results has two origins: 1) calculation of the equivalent damping and the effective stiffness of the NLASDs; 2) the analysis method applied. The uncertainty of the ELA method using SDOF system is well-discussed in Section 3.1.2, while in Section 3.2 it is shown that the bending moments of the piers obtained with MMRSA or LTHA differ with up to 15% even in the longitudinal direction, which is assumed to behave as an SDOF system. This difference is even higher, 39% in the transverse direction, which is responsible for the high uncertainty of the results.

As a conclusion, considering a factor of 1.3 for the increase of the internal forces due to the uncertainty of the results of the ELA seems to be a rational choice, since conservative results are obtained in both directions. However, NLTHA of the last configuration has to be carried out for validation.

8 Conclusions

In this paper possible retrofit versions of the existing large-span highway bridge over the Danube river at Háros, Hungary are investigated. The bridge was built in 1990 without any seismic consideration in design; however, the state-of-the-art studies on seismicity of Hungary indicates that the bridge is situated in a moderate seismicity area. Seismic modal response spectra analysis is carried out in accordance with EC8-2, and the results

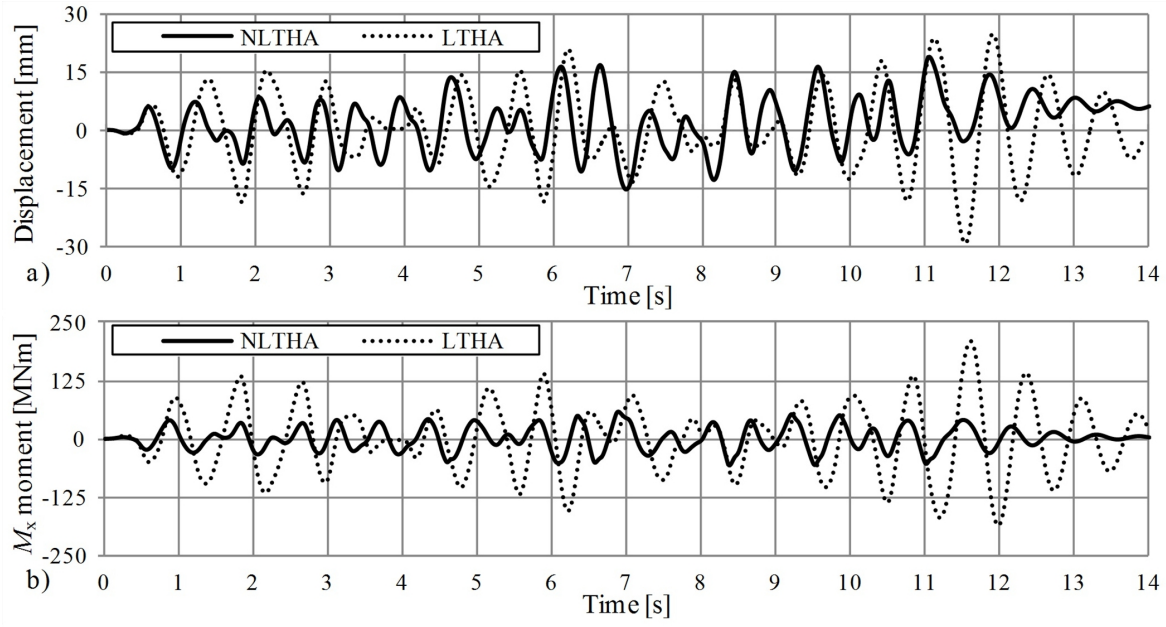

Fig. 12. Comparison of results from LTHA of the original (version V1) and NLTHA of the final retrofitted configuration (version V9) using the same #R1 artificial record. (a): longitudinal displacements [mm] of the river bridge girder; (b): M_x (longitudinal bending moments) [MNm] in the most critical pier P5.

indicate the seismic vulnerability of the bridge in spite of the low peak ground acceleration level of 1.0 m/s^2: failure of piers and foundation can be expected, confirmed by the extremely high calculated D/C ratios approaching a value of 4.

The main goal is to avoid expensive strengthening methods such as strengthening the piers and foundations which are immersed in the river, thus methods that mitigate the seismic responses to a desired level are preferred. Various seismic demand mitigation methods – rearrangement of bearings, application of seismic devices and seismic isolator systems – are compared in the framework of parametric study for conceptual design.

In order to save computational time during the conceptual design of the reconstruction, linear MMRSA is used with effective dynamic properties assigned. The application of this method, however is limited if non-linear elements such as seismic isolator units are applied. Our case studies confirmed that the accuracy of the existing formula for the determination of the effective damping ratio provided by EC is not sufficient, the damping ratio is overestimated in several cases, thus this formula should be revised and modified. The approximation error of the EL method could be as high as 20 - 30% in case of high A_p / V_p ratios.

The discussed results of the parametric study well illustrate the effectiveness of the different systems and the evolution to reach an optimal configuration. It is concluded that sufficient reduction of internal forces of the critical members can be achieved neither by advanced dynamic analysis (LTHA and NLTHA) of the original configuration, nor rearrangement of the bearing system. Involvement of additional piers yields to drastically increased global base shear force, which could be not resisted by the higher number of load resisting members involved. Thus, despite the moderate seismicity, efficient quasi-elastic system avoiding strengthening of the existing members cannot be designed.

An optimal design is found to mitigate the seismic demands via the application of complex anti-seismic system. The determined optimal system involves non-linear anti-seismic (e.g. displacement dependent) devices replacing fixed bearings in the longitudinal and transverse direction as well as shock transmission units. Characteristics of the applied devices is determined in alignment with the actual stiffness and resistance of the critical members. Thus the developed system modifies the basic dynamic parameters (stiffness, fundamental period, damping) of the initial configuration and effectively limits the internal forces transferred from the superstructure to the critical substructure members.

NLTHA is also completed for the non-linear system in order to characterize the accuracy of the conceptual ELA. Comparison of NLTHA and ELA confirms that behavior of a non-linear – isolated – system can be well estimated in both longitudinal and transverse directions in spite of the fact that the system is multi-degree-of-freedom system. Although good estimation of the major seismic measures can be achieved by ELA, the results are typically non-conservative: ELA may underestimate the occurring forces in the system. NLTHA results provide a solid base for quantification of the observed error and a multiplication safety factor of 1.3 for the ELA method could be determined. The comparison of the two analysis methods shows that the effective stiffness method gives the designer adequate results for optimal retrofit decisions, but the limitations should be taken into account and the final version should be analyzed and checked by NLTHA as well for safe results.

Tab. 6. Comparison of ELA and NLTHA results.

Longitudinal direction									
Pier #		P5			P6			P7	
Param.	EL	NLTH	Δ%	EL	NLTH	Δ%	EL	NLTH	Δ%
F_{NLASD}	1401	1397	**0.3**	1386	1384	**0.1**	1380	1372	**0.6**
d_{NLASD}	18.1	14.5	**24.8**	17.1	13.7	**24.8**	16.8	12.8	**31.3**
d_{girder}	25.1	21.5	**16.5**	25.5	20.8	**22.6**	24.6	20.0	**23.0**
$d_{piertop}$	7.0	8.8	**-20.5**	8.4	9.0	**-6.7**	7.8	8.8	**-11.4**
M_{pier}	51.47	65.58	**-21.5**	50.77	63.93	**-20.6**	47.52	59.72	**-20.4**
Transverse direction									
Pier #		P5			P6			P7	
Param.	EL	NLTH	Δ%	EL	NLTH	Δ%	EL	NLTH	Δ%
F_{NLASD}	5136	4247	**20.9**	4633	4226	**9.6**	1456	1542	**-5.6**
d_{NLASD}	2.6	2.1	**23.8**	2.1	1.9	**10.5**	2.0	2.1	**-4.9**
d_{girder}	6.2	5.1	**21.6**	5.7	5.5	**3.6**	5.0	5.6	**-10.7**
$d_{piertop}$	3.6	3.1	**16.1**	3.6	3.6	**0.0**	3.1	4.1	**-25.6**
M_{pier}	108.39	93.59	**15.8**	97.99	93.29	**5.0**	61.99	68.40	**-9.4**

Note: F_{NLASD} – occurring internal force of NLASD [kN];
d_{NLASD} – deformation of NLD [mm];
d_{girder} – girder displacement [mm];
d_{pier} – pier top displacement [mm];
M_{pier} – pier bending moment [MNm].

Δ shows the difference in % between the EL and NLTHA results. For instance, the difference in the occuring internal forces (F_{NLASD}) in the longitudinal direction at pier P5 is calculated as follows: (1401 - 1397) / 1401 · 100% = 0.3%.

Acknowledgement

This paper was supported by the János Bolyai Research Scholarship of the Hungarian Academy of Sciences.

References

1 *EN 1998-1:2008 Eurocode 8: Design of structures for earthquake resistance – Part 1: General rules, seismic actions and rules for buildings*, European Committee for Standardization (CEN), 2008.

2 *EN 1998-1:2008 Eurocode 8: Design of structures for earthquake resistance – Part 2: Bridges*, European Committee for Standardization (CEN), 2008.

3 **Tóth L, Győri E, Mónus P, Zsíros T**, *Seismic hazard in the Pannonian region*, In: The Adria Microplate: GPS Geodesy, Tectonics and Hazards, Nato Science Series: IV: Earth and Environmental Sciences, Vol. 61, Springer Verlag, 2006, pp. 369-384, http://link.springer.com/chapter/10.1007/1-4020-4235-3_25, DOI 10.1007/1-4020-4235-3_25.

4 **Vigh LG, Dunai L, Kollár L**, *Numerical and design considerations of earthquake resistant design of two Danube bridges*, First European Conference on Earthquake Engineering and Seismology (Geneva, Switzerland), In:, pp. 1-10. Paper 1420.

5 **Simon J, Vigh LG**, *Seismic assessment of an existing Hungarian highway bridge*, Acta Technica Napocensis - Civil Engineering and Architecture, **56**(2), (2013), 43-57, http://constructii.utcluj.ro/ActaCivilEng/download/atn/ATN2013(2)_4.pdf.

6 **Zsarnóczay Á, Vigh LG, Kollár LP**, *Seismic Performance of Conventional Girder Bridges in Moderate Seismic Regions*, International Journal of Bridge Engineering, **19**(5), (2014), 1-9, DOI 10.1061/(ASCE)BE.1943-5592.0000536. Paper 04014001.

7 *Útügyi Műszaki Előírás ÚT 2-3.401 Közúti hidak tervezése, Általános előírások*, Magyar Útügyi Társaság, 2004.

8 **Iwan WD, Gates NC**, *The effective period and damping of a class of hysteretic structures*, Earthquake Engineering and Structural Dynamics, **7**, (1979), 199-211.

9 **Hwang JS, Sheng LH**, *Effective stiffness and equivalent damping of base isolated bridges*, Journal of Structural Engineering, **119**(10), (1993), 3094-3101.

10 **Hwang JS**, *Evaluation of equivalent linear analysis methods of bridge isolation*, Journal of Structural Engineering, **122**(8), (1996), 972-976.

11 **Hwang JS, Chang KC, Tsai MH**, *Composite damping ratio of seismically isolated regular bridges*, Engineering Structures, **19**(1), (1997), 52-62.

12 **Franchin P, Monti G, Pinto PE**, *On the accuracy of simplified methods for the analysis of isolated bridges*, Earthquake Engineering and Structural Dynamics, **30**(3), (2001), 363-382.

13 **Dicleli M, Buddaram S**, *Comprehensive evaluation of equivalent linear analysis method for seismic-isolated structures represented by SDOF systems*, Engineering Structures, **29**, (2007), 1653-1663.

14 **Jara M, Jara JM, Olmos BA, Casas JR**, *Improved procedure for equivalent linearization of bridges supported on hysteretic isolators*, Engineering Structures, **35**, (2012), 99-106.

15 **Simon J, Vigh LG**, *Response spectrum analysis of girder bridges with seismic isolators using effective stiffness*, WASET 2013 World Academy of Science, Engineering and Technology: International Conference on Civil, Structural and Earthquake Engineering (Istanbul, Turkey), In:, pp. 1353-1362.

16 **Liu T, Zordan T, Briseghella B, Zhang Q**, *An improved equivalent linear model of seismic isolation system with bilinear behavior*, Engineering Structures, **61**, (2014), 113-126.

17 **Zordan T, Liu T, Briseghella B, Zhang Q**, *Improved equivalent viscous damping model for base-isolated structures with lead rubber bearings*, Engineering Structures, **75**, (2014), 340-352.

18 *EN 15129:2010 Anti-seismic devices*, European Committee for Standardization (CEN), 2010.

19 *Guide Specifications for Seismic Isolation Design*, American Association of State Highway and Transportation Officials (AASHTO), 2010.

20 **Jacobsen LS, Ayre RS**, *Engineering vibrations*, McGraw-Hill; New York, USA, 1958.

21 **Veletsos AS, Venture CE**, *Modal Analysis of Non-Classically Damped Linear Systems*, Earthquake Engineering and Structural Dynamics, **14**, (1986), 217-243.

22 **Raggett JD**, *Estimation of damping of real structures*, Journal of Structural Division, Proc. of the ASCE, **101**, (1975), 1823-1835.
23 **Feng MQ, Lee SC**, *Determining the effective system damping of highway bridges*, Department of Civil and Environmental Engineering, University of California; California, USA, 2009.
24 **Hwang JS, Chiou JM, Sheng LH, Gates JH**, *A refined model for base-isolated bridges with bi-linear hysteretic bearings*, Earthquake Spectra, **12**(2), (1996), 245-272.
25 **Hwang JS, Sheng LH, Gates JH**, *Practical analysis of bridges on isolation bearings with bi-linear hysteresis characteristics*, Earthquake Spectra, **10**(4), (1994), 705-727.
26 *MATLAB 2010b Documentation*, The MathWorks Inc., 2010.
27 *ANSYS Release 11.0 Documentation*, Ansys Inc., 2007.